ISSN : 0974 - 7486 Volume 13 Issue 1

Materials Science

An Indian Journal

Full Paper

MSAIJ, 13(1), 2015 [001-013]

Effect of alloying elements on structure, physicaland chemical properties of SnBiZn solder alloy

Abu Bakr El-Bediwi, Amira El-Shafei, Mustafa Kamal
Metal Physics Lab., Physics Department, Faculty of Science, Mansoura University, (EGYPT)
E-mail: baker_elbediwi@yahoo.com

ABSTRACT

The effect of adding alloying elements, (Cu, In, Al, Se and Ag), on microstructure, electrical resistivity, elastic modulus, internal friction, melting point, wetting and corrosion behavior of $Sn_{72}Zn_4Bi_{24}$alloy have been investigated. Melting point, elastic modulus, internal friction, contact angle and electrochemical parameters of $Sn_{72}Zn_4Bi_{24}$alloy varied after adding Cu, In, Al, Se and Ag contents. The $Sn_{70}Zn_4Bi_{24}In_2$alloy has lower melting point, elastic modulus and internal friction values. The $Sn_{70}Zn_4Bi_{24}Ag_2$alloy has lower contact angle, corrosion rateand corrosioncurrent. Adding Cu, Al, Se and Ag content improve mechanical and electrical properties of $Sn_{72}Zn_4Bi_{24}$ lead free solder alloy.

KEYWORDS

Microstructure;
Wetting properties;
Electrical resistivity;
Mechanical properties;
Electrochemical corrosion behavior;
Lead free solder alloys.

INTRODUCTION

Lead-free solders in commercial use may contain tin, copper, silver, bismuth, indium, zinc, antimony, and traces of other metals. Sn-Zn solder alloy containing about 9 wt. % zinc (eutectic composition) has been proposed as a lead-free solder material which is expected to be put into practical use for reflow soldering. Those Sn-Zn solder alloys have advantages such that a eutectic temperature of a tin-zinc alloy is equal to 199° C, closest to a eutectic point of a tin-lead alloy among Sn-based lead-free solder alloys and costs of raw materials of them are lower than those of the other lead-free solder alloys. The influence of adding cadmium content on structure and physical properties of $SnZn_9$ alloy has been investigated by El-Bediwi et al[1]. Also thermodynamic properties and phase equilibrium relationship of Sn-Bi-Zn lead free solder alloys are determined experimentally and theoretically by Yang et al[2]. Adding Ag to Sn-9Zn alloy inhibits the anodic dissolution of Zn and enhances the wettability of the solder alloy on Cu substrate[3]. The effect of RE elements on the microstructure, mechanical properties, wetting behavior of certain Pb-free solder alloys reported and summarized[4]. Several research[5-7] studied eutectic tin- silver lead free solder alloy. The results show that, the eutectic $SnAg_{3.5}$ is regarded as a good lead free solder alloy for certain aspects such as superior fatigue properties. Also

structure, electrical resistivity, wettability, melting point and elastic modulus of $Sn_{50}In_{50}$, $Sn_{72.2}In_{20}Ag_{2.8}$, $Sn_{72.5}In_{25}Ag_{2.5}$ and $Sn_{95}Ag_5$ lead free solder alloys have been investigated[8]. The results show that, adding silver decreased electrical resistivity and wetting and increase melting point and elastic modulus of tin-indium. Adding In from 0 to 3 wt. % to Sn-0.3Ag-0.7Cu lead-free solder alloy lowered its solidus and liquidus temperatures with increasing melting range. Also wetting time of alloy is reduced with increased wetting force by increasing In content[9]. Indium is a useful element to solve the problem of high melting point and low wettability of solder on Cu substrate[10, 11]. Microstructure, thermal properties, corrosion and oxidation resistance of Sn-9Zn-0.5Ag-1In solder alloy were studied[12]. Adding 1% of In to Sn-9Zn-0.5Ag alloy decreased melting point of alloy and enhanced adhesion strength of alloy on Cu substrate. Also Sn-In-Ag system offers several advantages such as good wettability[13, 14], good corrosion behavior[15]and very satisfying interaction with the substrate, especially with copper[16]. Many studies have been made on various solders alloy based on Sn, e.g., Sn-9Zn, Sn-3.5Ag, Sn-3Ag-0.5Cu, etc. as likely substitutes[17-19]. The properties of two lead free solder alloys, Sn-3.5%Ag-1%Zn and Zn-In, are described by M. Mc Cormack et al[20]. Solidification behaviors of Sn-9Zn-XAg lead-free solder alloys are examined[21].

The melting behavior, wetting characteristic, coefficient of thermal expansion, microstructure and interfacial reaction kinetics between Sn-Bi-Ag-(In) solders and Au/Ni metalized Cu substrate are studied by R. K. Shiue et al[22]. The Sn-Bi alloy has the highest ultimate tensile strength of all alloys examined, while both Sn–Ag and Sn–Zn alloys are lighter and exhibited higher ductility than the Sn-Pb and Sn-Bialloys[23]. Thermal properties and microstructure of 58% Bi-42% Sn, 53% Bi-26% Sn-21% Cd,70% In-30% Sn, 50% Sn-50% In and 3% Sn-37% Bi-10% In solder alloys have been studied and analyzed[24]. The thermodynamic properties and phase equilibrium relationship of Sn-Bi-Zn lead free solder alloys are determined experimentally and theoretically by Yang et al[25]. Microstructure, electrical, mechanical and thermal properties of rapidly solidified $Bi_{58}Sn_{42}$ eutectic alloy have been investigated using scanning electron microscope, x-ray, double bridge method, dynamic resonance technique and Vickers hardness tester[26]. The results show that, Bi-Sn eutectic alloy has a good soldering property such as low melting point, mechanical properties, adequate wettability and cost. The 69.5Sn-30Bi-0.5Cu exhibits good wettability on Cu substrate. Intermetallics formed at the 69.5Sn-30Bi-0.5Cu/Cu interface are identified as Cu_6Sn_5 adjacent to the solder and Cu_3Sn adjacent to the Cu substrate, respectively. Formation of intermetallic seems to improve strong wetting of the substrate by the solder[27]. A bismuth-silver alloy (Bi-11wt. %Ag) has been identified as a viable Pb-free power die-attach solder[28]. The alloy has a solidus at 262.5°C and a liquidus at 360°C. It has a shear modulus of 13.28 GPa and an ultimate tensile strength (UTS) of 59 MPa. The aim of this work is to improve\ or produce new alloy with superior properties by adding alloying elements to $Sn_{72}Zn_4Bi_{24}$alloy.

EXPERIMENTAL WORK

In the present work, $Sn_{72-x}Zn_4Bi_{24}X_x$(X=Ag, Al, Cu, Se and In and x=2 wt.%) were melted in a muffle furnace using tin, zinc, bismuth, copper, aluminum, indium, silver and selenium of purity better than 99.5 %. The resulting ingots were turned and re-melted four times to increase the homogeneity. From these ingots, long ribbons of about 4 mm width and ~70 μm thickness were prepared by a single roller method in air (melt spinning technique). The surface velocity of the roller was 31.4 m/s giving a cooling rate of $\sim 3.7 \times 10^5$ K/s. The samples then cut into convenient shape for the measurements using double knife cuter. Structure of used samples was performed on the flat surface of all samples using an Shimadzu X–ray Diffractometer (Dx–30, Japan)of Cu–Kα radiation with λ=1.54056 Å at 45 kV and 35 mA and Ni–filter in the angular range 2θ ranging from 0 to 100° in continuous mode with a scan speed 5 deg/min. Scanning electron microscope JEOL JSM-6510LV, Japan also was used to study microstructure**.** The electrical resistivity was measured by a conventional double bridge method. The differential thermal

analysis (DTA) thermographs were obtained by SDT Q600 V20.9 Build 20 instrument with heating rate 10 °k/min. The internal friction Q^{-1} and the elastic constants were determined using the dynamic resonance method. The value of the dynamic Young modulus Eis determined by the relationship[29–31]. The polarization studies were performed using Gamry Potentiostat/Galvanostat with a Gamry framework system based on ESA 300. Gamry applications include software DC105 for corrosion measurements, and Echem Analyst version 5.5 software packages for data fitting.

RESULTS AND DISCUSSION

X-ray analysis

X-ray diffraction patterns of $Sn_{72-x}Zn_4Bi_{24}X_x$ (X=Ag, Al, Cu, Se and In and x=2 wt.%) rapidly solidified alloys have lines corresponding to sharp lines of body-centered tetragonal Sn phaserhombohedral Bi phase and rhombohedral SnBi intermetallic phaseas shown in Figure 1. X-ray diffraction analysisfor $Sn_{72-x}Zn_4Bi_{24}X_x$alloys show that, they consisted of β-Sn phase, rhombohedralBi phase and rhombohedral SnBi intermetallic compound and that agreed with pervious results[32, 33]. That is mean Zn, Ag, Cu, In, Al and Se atoms dissolved in Sn matrix forming a solid solution with changingSn matrix microstructure of $Sn_{72}Zn_4Bi_{24}$alloy such as crystallinity (which is related to intensity of the peak), crystal size (which is related to full width half maximum), and orientation (which is related to the position of the peak, 2θ), after adding Ag, Cu, In, Al and Se contents. The details of x-ray analysis, (position, intensity, full width half maximum, area under the peak, miller indices), of $Sn_{72-x}Zn_4Bi_{24}X_x$ (X=Ag, Al, Cu, Se and In and x=2 wt. %) alloys are seen in TABLE 1.

Lattice parameters, (a and c), and unit volume cell of β- Sn for used alloys were determined[34]. The maxima of the diffraction pattern are broadened by an amount inversely proportional to the crystallite size and measurement of the additional broadening thus gives a means of estimating the size through the formula given by Scherer equation[35]. TABLE 2 shows the calculated lattice parameters, (a and c), unit volume cell and crystal size of body-centered tetragonal Sn phase in $Sn_{72-x}Zn_4Bi_{24}X_x$ (X=Ag, Al, Cu, Se and In and x=2 wt. %) alloys. From these results, lattice parameters, unit cell volume and crystal size of β-Sn phase in $Sn_{72}Zn_4Bi_{24}$alloy changed after adding Ag, Cu, In, Al and Se contents. That is because Ag, Cu, In, Al and Seatoms dissolved in matrix alloy.

Scanning electron microscope

Scanning electron micrographs, SEM, of $Sn_{72-x}Zn_4Bi_{24}X_x$ (X=Ag, Al, Cu, Se and In and x=2 wt. %) alloys are shown in Figure 2. SEM analysis of $Sn_{72-x}Zn_4Bi_{24}X_x$ alloys showed considerable heterogeneity of micro-structure, which will relate to the formation of non-equilibrium phases. Three types of phases, (β-Sn phase) or (β-Sn phase, Bi phase and SnBi intermetallic compound), of various chemical compositions were detected, which was also proved by the x-ray analysis.

Thermal properties

Wettability

Wettability is quantitatively assessed by the contact angle formed at the solder substrate's flux triple point. The contact angles of $Sn_{72-x}Zn_4Bi_{24}X_x$ (X=Ag, Al, Cu, Se and In and x=2 wt. %) alloys on pure Cu substrate are shown in TABLE 3. The results show that, adding Ag, Se and In content decreased contact angle of $Sn_{72}Zn_4Bi_{24}$ alloy but Cu and Al increased it as seen in TABLE 3. The $Sn_{70}Zn_4Bi_{24}Ag_2$alloy has lower contact angle, good wetting on pure Cu substrate. The spreading of $Sn_{72-x}Zn_4Bi_{24}X_x$alloys on pure Cu at room temperature in air is shown Figure 3.

Melting point

The melting temperature is an important physical property and has a great influence on printed circuit board assembly. A promising solder alloy should have a lower melting temperature and a narrow pasty temperature zone. Figure 4 shows the DSC thermographs of $Sn_{72-x}Zn_4Bi_{24}X_x$ (X=Ag, Al, Cu, Se and In and x=2 wt. %)alloys. The melting point of $Sn_{72-x}Zn_4Bi_{24}X_x$alloys is listed in TABLE 4. Thermographs, Exo-thermal peaks, of $Sn_{72-x}Zn_4Bi_{24}X_x$ alloys have a variation in their shape. That means that,

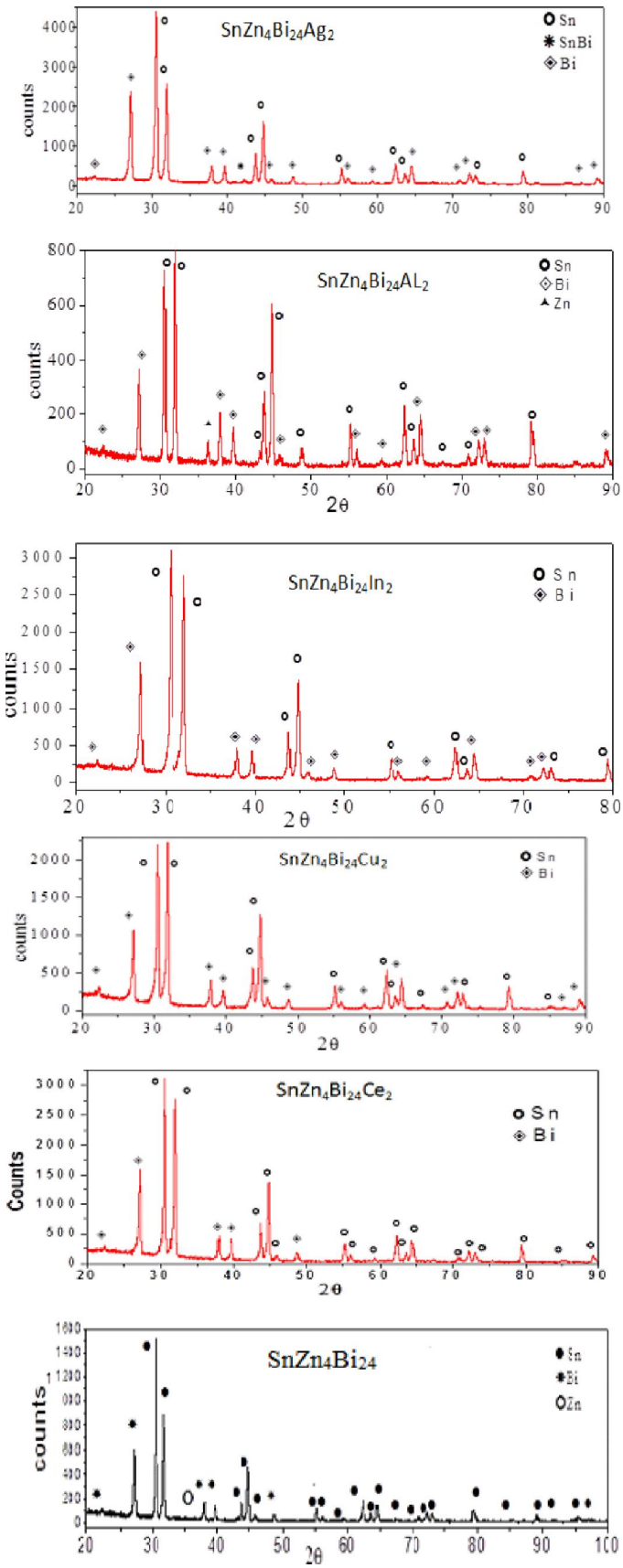

Figure 1 : x-ray diffraction patterns of Sn_{72-x} Zn_4X_xalloys

TABLE 1 : x-ray diffraction analysis of $Sn_{72-x}Zn_4X_x$ alloys$Sn_{70}Zn_4Bi_{24}Ag_2$

2θ	d Å	Int. %	FWHM	Area	Phase	hkl
22.3835	3.972	1.76	0.2362	16.72	Bi	003
27.1831	3.28061	50.88	0.2558	523.95	Bi	012
30.5759	2.92387	100	0.3149	1267.3	Sn	200
31.8964	2.80577	57.57	0.2755	638.41	Sn	101
37.8527	2.37685	9.53	0.1378	52.83	Bi	104
39.6124	2.27523	10.33	0.1181	49.11	Bi	110
42.2635	2.13844	1.36	0.3149	17.19	SnBi	220
43.7577	2.06882	17.78	0.1574	112.65	Sn	220
44.8289	2.02185	35.65	0.2165	310.57	Sn	211
45.7656	1.98262	1.85	0.3542	26.43	Bi	006
48.8009	1.86617	3.8	0.2755	42.15	Bi	202
55.1669	1.66495	8.58	0.2755	95.17	SnBi	400
55.97	1.64295	3.1	0.3149	39.24	Bi	024
59.2821	1.55882	1.15	0.3936	18.27	Bi	107
62.367	1.48893	11.23	0.3542	160.17	Sn	112
63.5824	1.46336	5.41	0.2755	59.94	Sn	400
64.3671	1.44741	8.93	0.3542	127.38	Bi	122
70.9309	1.32872	1.77	0.3149	22.44	Bi	009
72.1565	1.30914	5.67	0.1968	44.9	Bi	300
72.9667	1.29659	4.86	0.1968	38.49	Sn	411
79.2838	1.20839	7.38	0.2362	70.18	Sn	312
89.1627	1.09741	3.19	0.288	49.99	Bi	306
			$Sn_{70}Zn_4Bi_{24}Al_2$			
22.3851	3.97172	2.76	0.4723	9.41	Bi	003
27.1708	3.28206	42.56	0.2558	78.51	Bi	012
30.5323	2.92794	91.94	0.2558	169.62	Sn	200
31.9437	2.80173	100	0.2952	212.86	Sn	101
36.2676	2.47701	9.3	0.1968	13.2	Zn	002
37.9393	2.37162	20.23	0.2558	37.32	Bi	104
39.6495	2.27318	15.69	0.2362	26.72	Bi	110
43.1893	2.09473	4.78	0.1968	6.78	Sn	220
43.7447	2.06941	32.95	0.2755	65.47	Sn	220
44.8019	2.023	77.78	0.3346	187.64	Sn	211
45.852	1.97909	3.62	0.3149	8.22	Bi	006
48.7499	1.868	8.17	0.1968	11.59	Bi	202
55.1497	1.66543	18.49	0.1968	26.24	SnBi	400
56.0701	1.64025	6.43	0.2952	13.68	Bi	024
59.3313	1.55764	2.35	0.3542	6	Bi	107
62.3533	1.48922	24.26	0.2165	37.87	Sn	112
63.5912	1.46318	10.44	0.2558	19.25	Sn	400
64.4047	1.44665	22.56	0.2558	41.61	Bi	122
67.3851	1.38974	1.58	0.4723	5.36	Sn	321
70.8621	1.32984	4.09	0.2362	6.96	Bi	009

Full Paper

2θ	d Å	Int. %	FWHM	Area	Phase	hkl
72.0817	1.31031	9.76	0.2165	15.23	Bi	300
72.8795	1.29792	9.91	0.2165	15.46	Sn	411
79.2731	1.20853	20.54	0.2165	32.06	Sn	312
85.0508	1.14058	1.64	0.7872	9.29	Sn	431
89.1625	1.09742	6.67	0.24	15.61	Bi	306
			$Sn_{70}Zn_4Bi_{24}Cu_2$			
22.4394	3.96223	5.43	0.1968	22.42	Bi	003
27.1136	3.28886	43.57	0.1574	143.81	Bi	012
30.5285	2.9283	98.17	0.1968	404.99	Sn	200
31.9153	2.80183	100	0.144	408.01	Sn	101
37.9955	2.36629	12.5	0.192	68.02	Bi	104
39.6155	2.27317	9.75	0.336	92.8	Bi	110
43.7217	2.06873	23.84	0.168	113.49	Sn	220
44.8283	2.0202	54.76	0.336	521.31	Sn	211
45.7753	1.98058	5.81	0.24	39.53	Bi	006
48.7362	1.86695	5.37	0.384	58.41	Bi	202
55.213	1.66229	13.07	0.336	124.47	Sn	301
56.0515	1.63939	3.65	0.432	44.63	Bi	024
59.2849	1.55746	2.54	0.384	27.6	Bi	107
62.365	1.48774	21.08	0.12	71.68	Sn	112
63.6222	1.46133	6.56	0.288	53.5	Sn	400
64.3966	1.44562	17.09	0.288	139.46	Bi	122
67.4156	1.38803	1.73	0.384	18.85	Sn	321
70.7805	1.33007	3.16	0.192	17.21	Bi	009
72.156	1.30806	9.07	0.24	61.65	Bi	300
72.9048	1.29646	8.11	0.288	66.21	Sn	411
79.2803	1.20743	13.46	0.288	109.8	Sn	312
85.0713	1.13941	1.39	0.96	37.67	Sn	431
89.0912	1.09811	5.36	0.288	43.78	Bi	306
			$Sn_{70}Zn_4Bi_{24}In_2$			
22.4211	3.96543	4.06	0.1968	25.76	Bi	003
27.2342	3.27456	20.79	0.2558	171.62	Bi	012
30.5386	2.92735	100	0.2165	698.35	Sn	200
31.8934	2.80603	89.23	0.2558	736.4	Sn	101
38.0026	2.36782	8.94	0.2362	68.12	Bi	104
39.617	2.27497	6.1	0.1968	38.73	Bi	110
43.7321	2.06997	24.27	0.1574	123.24	Sn	220
44.7378	2.02575	47.39	0.1771	270.78	Sn	211
45.8019	1.98113	3.32	0.2362	25.32	Bi	006
48.7089	1.86948	2.89	0.2362	22	Bi	202
55.1586	1.66518	8.73	0.3149	88.7	SnBi	400
55.9715	1.64291	1.84	0.3149	18.64	Bi	024
59.2531	1.55951	1.21	0.3149	12.27	Bi	107
62.356	1.48916	12.98	0.1574	65.93	Sn	112
63.5815	1.46338	4.31	0.2755	38.3	Sn	400

2θ	d Å	Int. %	FWHM	Area	Phase	hkl
64.3349	1.44805	8.67	0.2362	66.04	Bi	122
70.8479	1.33007	1.11	0.2362	8.44	Bi	009
72.1955	1.30853	5.04	0.2362	38.4	Bi	300
72.9218	1.29727	4.97	0.1968	31.55	Sn	411
79.2867	1.20735	7.84	0.192	65.6	Sn	312
			$Sn_{70}Zn_4Bi_{24}Se_2$			
22.396	3.96981	2.1	0.2362	13.53	Bi	003
27.1618	3.28312	46.61	0.1574	200.47	Bi	012
30.5761	2.92385	100	0.1968	537.57	Sn	200
31.9332	2.80262	94.8	0.1771	458.65	Sn	101
37.8887	2.37468	13.61	0.1378	51.2	Bi	104
39.7178	2.26943	10.43	0.1378	39.27	Bi	101
43.7471	2.0693	21.74	0.1378	81.81	Sn	220
44.8162	2.02239	44.48	0.2165	263	Sn	211
45.8714	1.9783	2.41	0.3936	25.94	Sn	211
48.6857	1.87032	4.75	0.2755	35.79	Bi	202
55.1821	1.66452	9.98	0.2755	75.14	SnBi	400
56.0234	1.64151	3.19	0.1968	17.13	Sn	301
59.2185	1.56034	1.25	0.3149	10.79	Sn	301
62.4067	1.48808	15.03	0.1574	64.65	Sn	112
63.6114	1.46277	4.51	0.1968	24.26	Sn	400
64.3764	1.44722	10.39	0.2755	78.21	Sn	321
70.8403	1.33019	1.73	0.3149	14.86	Sn	420
72.1448	1.30932	4.69	0.2362	30.24	Sn	420
72.9676	1.29657	5.06	0.2362	32.64	Sn	411
79.2717	1.20854	7.49	0.1181	24.17	Sn	312
89.0772	1.09825	3.26	0.288	34.62	Sn	431
			$Sn_{70}Zn_4Bi_{24}$			
22.3734	3.97377	1.81	0.4723	12.11	Bi	003
27.1373	3.28603	35.75	0.2558	129.88	Bi	012
30.5711	2.92432	100	0.2362	335.39	Sn	200
31.9498	2.80121	54.51	0.2952	228.53	Sn	101
37.9358	2.37183	9	0.1968	25.16	Bi	104
39.6705	2.27203	7.9	0.2165	24.28	Bi	110
43.7703	2.06826	14.11	0.3149	63.09	Sn	220
44.7494	2.02525	27.6	0.2755	107.98	Sn	211
45.8756	1.97812	2.21	0.433	13.59	Sn	211
48.7508	1.86797	3.55	0.2362	11.90	Bi	202
55.3215	1.66066	6.86	0.2952	28.76	Sn	301
56.0971	1.63953	2.37	0.2362	7.96	Sn	301
59.3233	1.55784	1.02	0.4723	6.81	Sn	301
62.397	1.48828	10.63	0.1771	26.73	Sn	112
63.6275	1.46243	3.87	0.1968	10.81	Sn	400
64.4167	1.44641	7.85	0.2362	26.33	Sn	321
67.39	1.38965	1.04	0.09	1.35	Sn	321
70.8298	1.33037	1.94	0.2755	7.57	Sn	420
72.2064	1.30836	5.08	0.3149	22.70	Sn	420
72.8958	1.29767	3.18	0.2165	9.78	Sn	411
79.2482	1.20884	5.9	0.2165	18.15	Sn	312
89.1636	1.09832	3.27	0.1968	9.15	Sn	431
95.3488	1.04275	2.75	0.2165	8.46	Sn	332

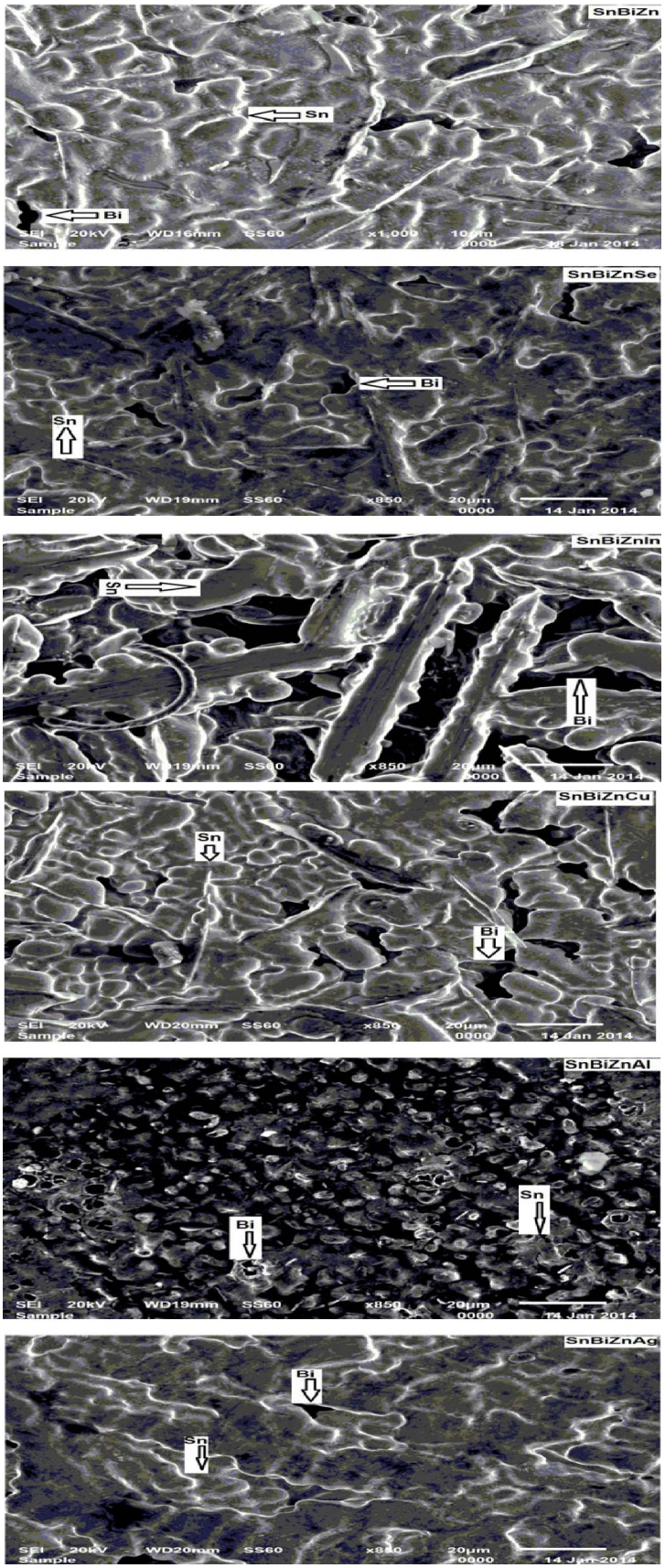

Figure 2 : SEM of $Sn_{72-x}Zn_4Bi_{24}X_2$alloys

TABLE 2 : lattice parameters and particle size of $Sn_{72-x}Zn_4X_x$ alloys

Alloys	τ(Å)	a (Å)	c (Å)	c/a	V (Å^3)
$Sn_{72}Zn_4Bi_{24}$	327.611	5.8497	3.194	0.546	109.295
$Sn_{70}Zn_4Bi_{24}In_2$	351.736	5.855	3.19	0.545	107.45
$Sn_{70}Zn_4Bi_{24}Se_2$	370.836	5.853	3.192	0.545	107.32
$Sn_{70}Zn_4Bi_{24}Ag_2$	306.202	5.852	3.194	0.546	107.201
$Sn_{70}Zn_4Bi_{24}Al_2$	304.679	5.856	3.19	0.545	107.49
$Sn_{70}Zn_4Bi_{24}Cu_2$	332.639	5.845	3.19	0.546	107.11

TABLE 3 : contact angles of $Sn_{72-x}Zn_4Bi_{24}X_x$alloys

Alloys	contact angle (θ)°
$Sn_{96}Zn_4$	23.5
$SnZn_4Bi_{24}$	29
$Sn_{70}Zn_4Bi_{24}Cu_2$	30
$Sn_{70}Zn_4Bi_{24}Ag_2$	26.5
$Sn_{70}Zn_4Bi_{24}Se_2$	28
$Sn_{70}Zn_4Bi_{24}Al_2$	35.5
$Sn_{70}Zn_4Bi_{24}In_2$	28

TABLE 4 : melting points of $Sn_{72-x}Zn_4Bi_{24}X_x$alloys

Alloys	Melting point °C
$Sn_{96}Zn_4$	
$SnZn_4Bi_{24}$	173.25
$SnZn_4Bi_{24}Al_2$	170.38
$SnZn_4Bi_{24}Se_2$	171.42
$SnZn_4Bi_{24}Cu_2$	170.48
$SnZn_4Bi_{24}In_2$	168.23
$SnZn_4Bi_{24}Ag_2$	185.98

TABLE 5 : electrical resistivity of $Sn_{72-x}Zn_4Bi_{24}X_x$alloys

Alloys	ρ x10 $^{-8}$ Ω^{-1}.m^{-1}
$Sn_{96}Zn_4$	36.08
$Sn_{72}Zn_4Bi_{24}$	68.83±6
$Sn_{70}Zn_4Bi_{24}In_2$	75.7±9
$Sn_{70}Zn_4Bi_{24}Se_2$	52.48±5.6
$Sn_{70}Zn_4Bi_{24}Ag_2$	54.3±7.5
$Sn_{70}Zn_4Bi_{24}Al_2$	63.7±9
$Sn_{70}Zn_4Bi_{24}Cu_2$	49.7±6

there is a change in alloys matrix structure caused after adding Ag, Cu, In, Al and Se contents to $Sn_{72}Zn_4Bi_{24}$ which agrees with the results seen in x-ray analysis and scanning electron micrographs. The melting temperature of $Sn_{72}Zn_4Bi_{24}$ alloy decreased after adding In, Cu, Al and Se contents. The $Sn_{70}Zn_4Bi_{24}In_2$ alloy has low melting point, 168°C, and it is lower than that the melting point of eutectic Sn-Pb solder alloy.

Electrical resistivity

In general, the plastic deformation raises the electrical resistivity as a result of the increased number of electron scattering centers. Crystalline defects serve as scattering center for conduction electrons in metals, so the increase in their number raises the

Full Paper

TABLE 6 : Elastic moduli, internal friction and thermal diffusivity of $Sn_{72-x}Zn_4Bi_{24}X_x$ alloys

Alloys	E GPa	B GPa	GPaμ	Q^{-1}	D_{th} x10^{-4} cm^2/sec
$Sn_{72}Zn_4Bi_{24}$	27.43	30.15	10.17	0.041	1.85
$Sn_{70}Zn_4Bi_{24}In_2$	24	26.7	8.88	0.013	2.52
$Sn_{70}Zn_4Bi_{24}Ag_2$	39.4	43.4	14.6	0.023	2.93
$Sn_{70}Zn_4Bi_{24}Cu_2$	40.9	44.8	15.2	0.046	2.03
$Sn_{70}Zn_4Bi_{24}Se_2$	33.3	36.4	12.3	0.046	2.06
$Sn_{70}Zn_4Bi_{24}Al_2$	30.1	33.1	11.1	0.057	1.25

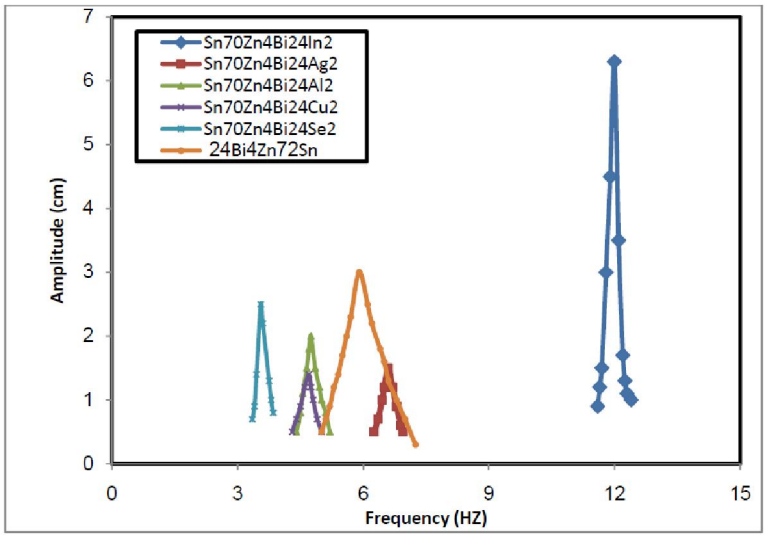

Figure 5 : Resonance curves of $Sn_{72-x}Zn_4Bi_{24}X_x$alloys

TABLE 7 : Corrosion current, corrosion potential and corrosion rate of $Sn_{72-x}Zn_4Bi_{24}X_x$ alloys

Alloys	I_{corr} x10^{-6}A	E_{corr} V	C.Rmpy
$SnZn_4Bi_{24}$	727	-0.954	332
$SnZn_4Bi_{24}Ag_2$	125	-0.517	129.8
$SnZn_4Bi_{24}Se_2$	1890	-0.1000	1964
$SnZn_4Bi_{24}Cu_2$	845	-0.974	879.2
$SnZn_4Bi_{24}Al_2$	154	-0.838	160.3
$SnZn_4Bi_{24}In_2$	6490	-0.977	2967

imperfection. The measured electrical resistivity of $Sn_{72-x}Zn_4Bi_{24}X_x$ (X=Ag, Al, Cu, Se and In and x=2 wt. %)alloys are listed in TABLE 5. Electrical resistivity of $Sn_{72}Zn_4Bi_{24}$ alloy decreased after adding Ag, Cu, Al and Se contents.

Elastic properties

The elastic constants are directly related to atomic bonding and structure. It is also related to the atomic density. Elastic moduli of $Sn_{72}Zn_4Bi_{24}$ alloy increased afterAg, Cu, Al and Se contents as shown in TABLE 6. The resonance curves of $Sn_{72-x}Zn_4Bi_{24}X_x$ (X=Ag, Al, Cu, Se and In and x=2 wt. %)alloys are shown in Figure 5. Calculated Internal friction and thermal diffusivity are seen in TABLE 6. The results show that, internal friction value of $Sn_{72}Zn_4Bi_{24}$alloy increased after adding Cu, Al and Se contents but it's decreased after adding In and Ag contents.

Electrochemical corrosion behavior

Figure 6 shows electrochemical polarization curves for $Sn_{72-x}Zn_4Bi_{24}X_2$ (X=Cu, In, Ag, Se and Al) alloys in 0.5M HCl. From this Figure, the corrosion potential of these alloys exhibited a negative potential. Also, the cathodic and the anodic polarization

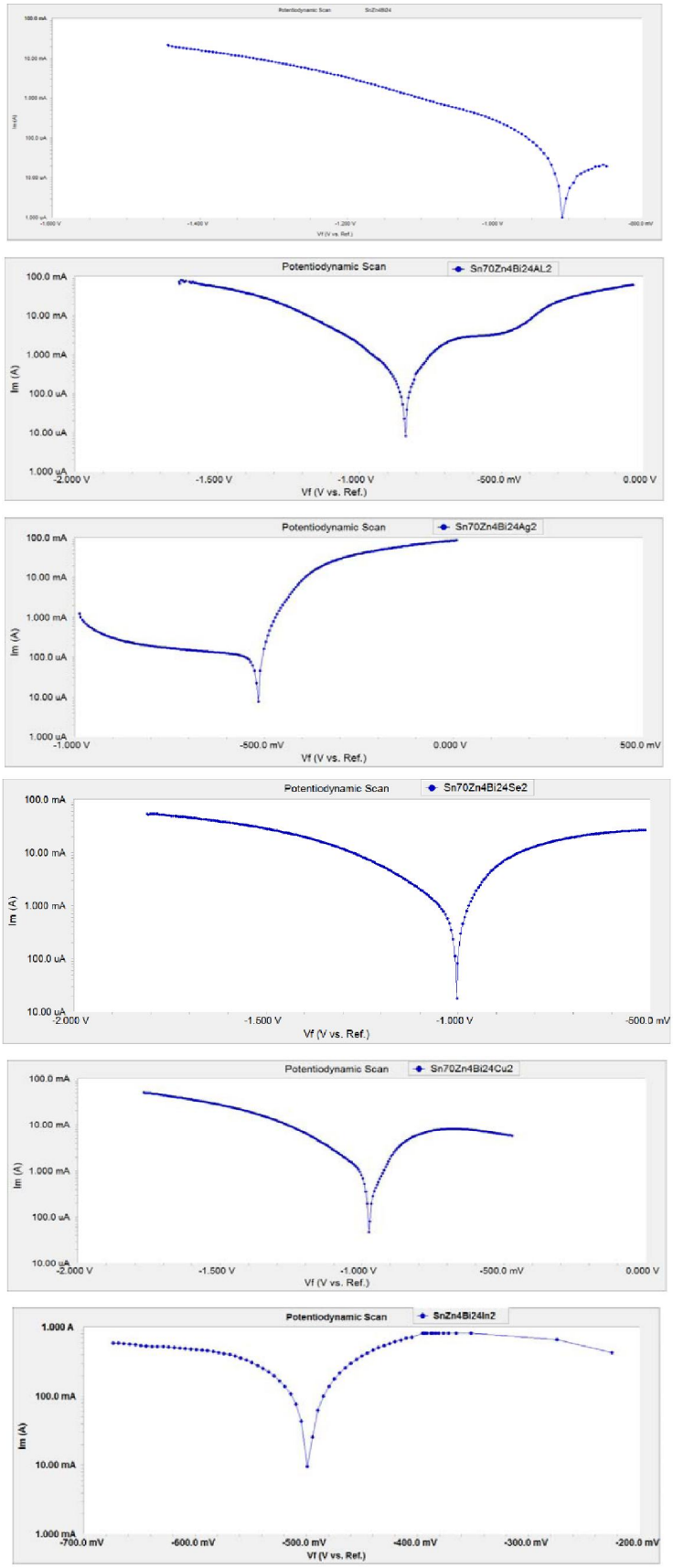

Figure 6 : Electrochemical polarization curves for $Sn_{72-x}Zn_4Bi_{24}X_2$alloys

Full Paper

curves showed similar corrosion trends. The corrosion potential (E_{Corr}), corrosion current (I_{Corr}), and corrosion rate (C. R) of $Sn_{72-x}Zn_4Bi_{24}X_2$ (X=Cu, In, Ag, Se and Al) alloys in 0.5M HCl are listed in TABLE 7. The results show that, corrosion parameters of $Sn_{72}Zn_4Bi_{24}$ alloy changed after adding Cu, In, Ag, Se and Al contents. That is because adding Cu, In, Ag, Se and Alto $Sn_{72}Zn_4Bi_{24}$alloy caused microstructure changed which affected on microsegregation and the reactivity of formed phases and other atoms with HCl solution. The $Sn_{70}Zn_4Bi_{24}Ag_2$alloy has lower corrosion current (I_{Corr}), and corrosion rate (C. R).

CONCLUSION

$Sn_{72-x}Zn_4Bi_{24}X_x$alloys consisted of β-Sn phase, rhombohedralBi phase and rhombohedral SnBi intermetallic compound. Also Zn, Ag, Cu, In, Al and Se atoms dissolved in Sn matrix of $Sn_{72}Zn_4Bi_{24}$alloychangingits microstructuresuch as forming a solid solution with changed crystallinity, crystal size, and orientation after adding Ag, Cu, In, Al and Se contents.

Electrical resistivity of $Sn_{72}Zn_4Bi_{24}$ alloy decreased after adding Ag, Cu, Al and Se contents.

Elastic moduli of $Sn_{72}Zn_4Bi_{24}$ alloy increased after Ag, Cu, Al and Se contents.

The $Sn_{70}Zn_4Bi_{24}Ag_2$alloy has lower corrosion current (I_{Corr}), and corrosion rate (C. R).

Internal friction of $Sn_{72}Zn_4Bi_{24}$alloy increased after adding Cu, Al and Se contents but it's decreased after adding In and Ag contents.

The melting temperature of $Sn_{72}Zn_4Bi_{24}$ alloy decreased after adding In, Cu, Al and Se contents. The $Sn_{70}Zn_4Bi_{24}In_2$ alloy has low melting point, 168°C, and it is lower than that the melting point of eutectic Sn-Pb solder alloy.

Contact angle of $Sn_{72}Zn_4Bi_{24}$ alloy decreased after adding Ag, Se and In contents but Cu and Al increased it. The $Sn_{70}Zn_4Bi_{24}Ag_2$alloy has lower contact angle, good wetting on pure Cu substrate.

REFERENCES

[1] A.El-bediwi, M.M.El-Bahay, M.Kamal; Radia.Eff.Def.in Sol., **159**, 491 **(2004)**.

[2] C.Yang, F.Chen, W.Gierlotka, S.Chen, K.Hsieh, L.Huang; Mater.Chem.Phys., **112**, 94 **(2008)**.

[3] T.Takemoto, T.Funaki, A.Matsunawa; J.Jap.Weld.Soc., **17**, 251 **(1999)**.

[4] C.M.L.Wu, D.Q.Yu, C.M.T.Law, L.Wang; Mater.Sci.Eng.: R: Reports, **44(1)**, 1 **(2004)**.

[5] Y Kariya, M.Otsuka; J.Electron.Mater, **27**, 866 **(1998)**.

[6] W.J.Tomlinson, A.Fullylove; J.Mater.Sci., **27**, 5777 **(1992)**.

[7] F.Ochoa, J.J.Williams, N.Chawla; J.Electron Mater., **32**, 1414 **(2003)**.

[8] A.El-Bediwi, M.M.El-Bahay; Radia.Eff.Def.in Sol., **159**, 133 **(2004)**.

[9] K.Kanlayasiri, M.Mongkolwongrojn, T.Ariga; J.of alloys, compounds, **485**, 225 **(2009)**.

[10] M.S.Yeh; J.Electron.Mater., **30**, 953 **(2002)**.

[11] S.P.Yu, C.L.Liao, M.C.Wang, M.H.Hon; J.Mater.Sci., **35**, 1 **(2001)**.

[12] T.C.Chang, J.W.Wang, M.C.Wang, M.H.Hon; J.alloys & Comp., **(2006)**.

[13] D.R.Frear; j.Metals, **48(5)**, 49 **(1996)**.

[14] I.Artaki, A.M.Jackson, P.T.Vianco; J.Electron.Mater., **23(8)**, 757 **(1994)**.

[15] H.Oulfajrite, A.Sabbar, M.boulghallat, A.Touaiti, R.Lbibb, A.zrineh; Mater.Lett., **57**, 4368 **(2003)**.

[16] W.K.Choi, H.M.Lee, J.Korean., Phys.Soc., **35**, 340 **(1999)**.

[17] R.K.Shiue, L.W.Tsay, C.L.Lin, J.L.Ou; J.Mater.Sci., **38**, 1269 **(2003)**.

[18] A.Miiyamoto, T.Ogawa, T.Ohsawa; Mater.Sci.Res.Inter., **9**, 16 **(2003)**.

[19] A.B.El-Bediwi, M.El-Sayed, M.Kamal; Radia.Eff.Def.in Sol., **160(7)**, 297 **(2005)**.

[20] M.Mc Cormack, S.Jin, G.W.Kammlott, H.S.Chen; Appl.Phys.Lett., **63**, 15 **(1993)**.

[21] Y.L.Tsai, W.S.Hwang; Material Science and Engineering A, **312**, 413-414 **(2005)**.

[22] R.K.Shiue, L.W.Tsay, C.L.Lin, J.L.Ou; J.Mater.Sci., **38**, 1269 **(2003)**.

[23] W.R.Osório, L.C.Peixoto, L.R.Garcia, N.M.Noël, A.Garcia; *J.of Alloys and compounds, **572**, 97 **(2013)***.

[24] J.Chriastelova, M.Ozvold; J.of alloys and compounds, **457**, 323 **(2008)**.

[25] C.Yang, F.Chen, W.Gierlotka, S.Chen, K.Hsieh, L.Huang; Mater.Chem.Phys., **112**, 94 **(2008)**.

[26] M.Kamal, S.Mazen, A.El-Bediwi, E.Kashita; Radia.Eff.Def.in Sol., **161**, 143 **(2006)**.

[27] L.Zanga, Z.Yuan, H.Zhao, X.Zhang; Mater.Lett., **63**, 2067 **(2009)**.
[28] J.N.Lalena, N.F.Dean, M.W.Weiser; J.Electronic Mater, **31**, 11 **(2002)**.
[29] E.Schreiber, O.L.Anderson, N.Soga; "Elastic constant and their measurements", McGraw-Hill, New York, **82, (1973)**.
[30] S.Timoshenko, J.N.Goddier; "Theory of elasticity, 2nd Edition", McGraw- Hill, New York, **277, (1951)**.
[31] K.Nuttall; J.Inst.Met., **99**, 266 **(1971)**.
[32] J.Zhou, Y.Sun, F.Xue; J.Alloys Compd., **397**, 260 **(2005)**.
[33] S.W.Chen, C.H.Wang, S.K.Lin, C.N.Chiu; J.Mater.Sci.: Mater.Electron., **18**, 19 **(2007)**.
[34] Tables for X-Ray Crystallography, **1**, 15-21 **(1952)**.
[35] B.D.Cullity; "Element of x-ray diffraction" **10**, 297 **(1959)**.
[36] A.Mulugeta, S.Guna; Mater.Sci.Eng., **27**, 95 **(2000)**.
[37] L.C.Prasad, A.Mikula; J.Alloys Compd., **282**, 279 **(1999)**.
[38] D.Soares, C.Vilarinho, J.Barbosa, R.Silva, F.Castro; IX conference on metallurgical science and technology, Madrid, November, 5-7 **(2003)**; **1**-Tables for X-Ray Crystallography, **1**, 15-21 **(1952)**; **2**-B.D.Cullity "Element of x-ray diffraction", **10**, 297 **(1959)**.